THE JOURNAL OF BIOLOGICAL CHEMISTRY VOL. 286, NO. 23, pp. 20194–20207, June 10, 2011

Hypoxia Induces an Increase in Intracellular Magnesium via Transient Receptor Potential Melastatin 7 (TRPM7) Channels in Rat Hippocampal Neurons *in Vitro*[*][S]

Received for publication, May 26, 2010, and in revised form, April 6, 2011 Published, JBC Papers in Press, April 12, 2011, DOI 10.1074/jbc.M110.148494

Jing Zhang[1], **Fengbo Zhao**[1], **Yin Zhao, Jing Wang, Lei Pei, Ning Sun, and Jing Shi**[2]

From the Department of Neurobiology and Key Laboratory of Neurological Disease of Hubei Province, Tongji Medical College, Huazhong University of Science and Technology, 13 Hangkong Road, Wuhan 430030, China

TRPM7, a divalent cation channel, plays an important role in neurons damaged from cerebral ischemia due to permitting intracellular calcium overload. This study aimed to explore whether magnesium was transported via a TRPM7 channel into the intracellular space of rat hippocampal neurons after 1 h of oxygen-glucose deprivation (OGD) and acute chemical ischemia (CI) by using methods of the Mg^{2+} fluorescent probe Mag-Fura-2 to detect intracellular magnesium concentration ($[Mg^{2+}]_i$) and flame atomic absorption spectrometry to measure extracellular magnesium concentration ($[Mg^{2+}]_o$). The results showed that the neuronal $[Mg^{2+}]_i$ was 1.51-fold higher after 1 h of OGD at a basal level, and the increase of neuronal $[Mg^{2+}]_i$ reached a peak after 1 h of OGD and was kept for 60 min with re-oxygenation. Meanwhile, the $[Mg^{2+}]_o$ decreased after 1 h of OGD and recovered to the pre-ischemic level within 15 min after re-oxygenation. In the case of CI, the $[Mg^{2+}]_i$ peak immediately appeared in hippocampal neurons. This increase of $[Mg^{2+}]_i$ declined by removing extracellular magnesium in OGD or CI. Furthermore, by using Gd^{3+} or 2-aminoethoxydiphenyl borate to inhibit TRPM7 channels, the $[Mg^{2+}]_i$ increase, which was induced by OGD or CI, was attenuated without altering the basal level of $[Mg^{2+}]_i$. By silencing TRPM7 with shRNA in hippocampal neurons, it was found that not only was the increase of $[Mg^{2+}]_i$ induced by OGD or CI but also the basal levels of $[Mg^{2+}]_i$ were attenuated. In contrast, overexpression of TRPM7 in HEK293 cells exaggerated both the basal levels and increased $[Mg^{2+}]_i$ after 1 h of OGD/CI. These results suggest that anoxia induced the increase of $[Mg^{2+}]_i$ via TRPM7 channels in rat hippocampal neurons.

Transient cerebral ischemia results in selective death of neurons in specific brain regions. The hippocampus is a brain region particularly sensitive to cerebral ischemia (1). Neuronal death in the brain results from a variety of pathophysiological changes related to ischemia, and the mechanism underlying it is mainly focused on Ca^{2+} overload (2). Ca^{2+} can gain access into cells through ion channels (3, 4) and Na^+/Ca^{2+} exchangers (5) and from internal stores (endoplasmic reticulum and mitochondria) (6, 7). The best investigated ion channels in ischemic stroke are *N*-methyl-D-aspartate and amino-3-hydroxy-5-methyl-4-isoxazole propionate receptor channels opened by glutamate, which played key roles in excitotoxic cell death (8). Nevertheless, clinical trials with drugs targeting these receptors have not been effective (9–11).

Increasing evidence suggests that there may be mechanisms of neurotoxicity that operate independently of or in parallel with excitotoxicity. Much attention has been paid to such mechanisms involving the transient receptor potential melastatin 7 (TRPM7) channel, which is a nonselective cation channel permeable to Ca^{2+} and Mg^{2+}. Suppressing TRPM7 expression prevented ischemic neuronal death *in vitro* (12) and *in vivo* (13). Previous results from our laboratory are consistent with others that have also shown the TRPM7 channel contributes to neuronal death after ischemia (14). This indicates that TRPM7 is an essential mediator of ischemic death. Although TRPM7 channels may be one of the pathways that mediate the intracellular Ca^{2+} overload in anoxia conditions (15), we cannot ignore the dynamic change and effect of Mg^{2+} that can also permeate through TRPM7 channels (16–18).

Until recently, very little was known about the mechanisms regulating cellular magnesium homeostasis, and processes involving transmembrane transport of magnesium had been investigated only at the functional level (19) but not at the pathological level. Although there are a lot of possible reasons to explain the variability in the reported efficacy of magnesium-treated rats subjected to cerebral ischemia ("effective" in Refs. 20, 21; "not effective" in Refs. 22, 23), the profile of intracellular magnesium changes during ischemia reperfusion and the possible involved mechanisms, which may be not only related to the application of magnesium but also may be explained by the pathology of cerebral ischemia, remain to be defined.

TRPM7, a unique protein, termed chanzyme because it possess a channel and α-kinase domain, has now been identified as a magnesium transporter (18). TRPM7 distributes ubiquitously. Functional TRPM7 channels are expressed in neuronal cells where they play important roles in brain ischemia conditions described above. Also, magnesium ions have been reported to permeate through TRPM7 channels in

* This work was supported by the National Natural Science Foundation of China Grant 30870793.
[S] The on-line version of this article (available at http://www.jbc.org) contains supplemental "Experimental Procedures," "Results," and Figs. 1–5.
[1] Both authors contributed equally to this work.
[2] To whom correspondence should be addressed. Tel.: 86-27-83650545; Fax: 86-27-83692608; E-mail: sj@mails.tjmu.edu.cn.

neurons (24). However, whether neuronal $[Mg^{2+}]_i$[3] changes during the anoxia conditions and whether TRPM7 channels play a role in neuronal magnesium dynamic movement in physiological or ischemic levels have never been checked. Therefore, using the classic models of cerebral ischemia injury *in vitro*, we investigated the effects of oxygen-glucose deprivation and acute chemical ischemia on the magnesium dynamic movement in rat hippocampal neurons and HEK293 cells and explored the possible pathway-TRPM7 channel.

EXPERIMENTAL PROCEDURES

Cell Culture—Rat hippocampal neurons were cultured as described previously (25). The protocol for the use of rats for neuronal cultures was performed according to the principles of the Animal Care Committee of Chinese Academy of Medical Sciences.

Briefly, neonatal rats (within 1 day) were decapitated, and the hippocampus was isolated under a dissection microscope, cut into about 1-m^3 volume pieces, and incubated with 0.25% trypsin/EDTA for 15 min at 37 °C. Freshly prepared DMEM/F-12 medium containing 10% fetal bovine serum (Invitrogen) was used to end the digestion procedure. Fire-polished glass pipettes were taken to gently triturate the tissue mass into the cell suspension. Finally, cells were counted and plated in poly-L-lysine-coated culture dishes or coverslips in 24-well plates at a density of 1×10^6 cells per dish or 2×10^5 cells per well, respectively. Neurons were maintained at 37 °C in a humidified 5% CO_2 atmospheric incubator. After 24 h, the culture medium was changed totally with Neurobasal medium supplemented with 2% B-27 (Invitrogen), and cultures were fed twice a week. Neurons were used for the experiments between days 11 and 14 *in vitro*.

Human embryonic kidney (HEK293) cells, with inducible expression of TRPM7 channels (HEK and TRPM7 cells), were cultured in DMEM supplemented with 10% fetal bovine serum and antibiotics (26). For the induction of TRPM7, the cells were treated with 1 μg/ml tetracycline, as described previously (26).

Drugs and Solutions—The control solution ECF contained (in mM) the following: 140 NaCl, 5.4 KCl, 2 $CaCl_2$, 1 $MgCl_2$, 33 glucose, 20 HEPES (pH 7.4) (adjusted with NaOH, and 320–335 mosM with sucrose). OGD was performed with glucose-free ECF containing (in mM) the following: 140 NaCl, 5.4 KCl, 2 $CaCl_2$, 1 $MgCl_2$, 33 *N*-methyl-D-glucamine and 20 HEPES (pH 7.4) (320–335 mosM). Mg^{2+}-free ECF had no added $MgCl_2$. Mg^{2+}-free internal solution contained (in mM) the following: CsCl 140, CsOH 35, HEPES 10, tetraethylammonium 2, EGTA 5, $CaCl_2$ 1 (pH 7.3) (300 mosM). External solution contained (in mM) the following: NaCl 140, KCl 5.4, $CaCl_2$ 1.3, HEPES 25, glucose 33 (pH 7.4) (330 mosM). Stocks of Mag-Fura-2 acetoxymethyl ester (Mag-Fura-2/AM; Invitrogen), $GdCl_3$, 2-APB, nimodipin, and digitonin (Sigma) were prepared in DMSO. Tetrodotoxin (Sigma) KCN stocks were prepared in distilled water. All were stored at −20 °C until used. All compounds were diluted to their final concentrations directly in the experimental solution. 10 μM $GdCl_3$ or 100 μM 2-APB was used to inhibit TRPM7 channels.

Oxygen-Glucose Deprivation—The cultures were transferred to an anaerobic incubator containing 5% CO_2 and 95% N_2 atmosphere (27). They were washed three times with 500 μl of glucose-free ECF solution and maintained anoxic (5% CO_2, 95% N_2) for 1 h at 37 °C. OGD was terminated by washing the cultures with oxygenated glucose-containing ECF solution. The cultures were maintained for a further appropriate duration at 37 °C in a humidified 5% CO_2 atmosphere.

Acute Chemical Ischemia—3 mM KCN was added to the glucose-free extracellular solutions to mimic the state of ischemia.

Measurement of Magnesium Concentration—After 11 days in culture, neurons were loaded with 5 μM Mag-Fura-2/AM, which is membrane-permeant, by incubation of glass coverslips with adhered neurons for 25 min at 37 °C. After incubation, the cells were washed three times in the recording medium at room temperature and incubated for another 20 min for complete hydrolysation of acetoxymethyl ester. Cells were washed and stored in the dark at room temperature until required. Vaseline was used to adhere the coverslip to the recording chamber. The chamber consisted of a stainless steel carrier with a well of 0.5 ml and a center opening to hold the round coverslip. The same protocol was applied in HEK293 cells, which were cultured to 60–70% confluence.

Single cells, loaded with Mag-Fura-2, were imaged using an inverted fluorescence microscope equipped with a fluor ×40 oil objective (NA = 0.90) (OLYMPUS IX71, Germany). Determination of $[Mg^{2+}]_i$ was performed using a dual-wavelength technique by using a poly-wavelength launcher (PolychromeV, TILL Photonics, Germany). The cells were alternately illuminated with light of 350 and 385 nm at a rate of 0.2 Hz with a chopper wheel, and fluorescence emission was measured at 510 nm. Excitation scans were routinely done over an area containing 3–5 cells. Time-dependent changes in emission fluorescence were measured in response to excitation and recorded by the TTVISION software.

The ratio of Mag-Fura-2 fluorescence intensities measured with excitation at 350 and 385 nm ($R_{F350/F385}$) was used as a $[Mg^{2+}]_i$-related signal. Basal $[Mg^{2+}]_i$ was calculated from the basal R of Mag-Fura-2 measured at the first 60 s of each experiment. Taking Mg^{2+}-free ECF solution as a standard, all values of the measured R were normalized to the standard R value taken with identical optics and were converted to $[Mg^{2+}]_i$ with the standard Equation 1,

$$[Mg^{2+}]_i = K_D \times (R - R_{min})/(R_{max} - R) \quad \text{(Eq. 1)}$$

where R_{min} and R_{max} are the R values at zero $[Mg^{2+}]_i$ and saturating $[Mg^{2+}]_i$, respectively, and K_D is the dissociation constant.

Cells were permeabilized with 10 μM digitonin in the presence of 50 mM magnesium to obtain maximal fluorescence

[3] The abbreviations used are: $[Mg^{2+}]_i$, intracellular magnesium concentration; $[Mg^{2+}]_o$, extracellular magnesium concentration; $[Ca^{2+}]_i$, intracellular calcium concentration; 2-APB, 2-aminoethoxydiphenyl borate; CI, chemical ischemia; ECF, extracellular fluid; EGFP, enhanced GFP; HEK, human embryonic kidney; KCN, potassium thiocyanate; OGD, oxygen glucose deprivation; Re, reperfusion; Tet(−) cells, HEK293 cells in the absence of induced expression of TRPM7 channels; Tet(+) cells, HEK293 cells induced expression of TRPM7 channels.

(R_{max}) of the Mag-Fura-2·Mg^{2+} complex. This was washed once, followed by the addition of 50 mM EDTA and 20 mM Tris buffer (pH 8.5) to determine R_{min} values. Free Mg^{2+} was determined as described previously (28, 29) using a K_D of 1.45 mM for the Mag-Fura-2·Mg^{2+} complex. $R_{max} = 0.86$ and $R_{min} = 0.268$.

Flame Atomic Absorption Spectrometry—We used a Varian AA240FS fast sequential atomic absorption spectrometer. 50 μl of extracellular liquid according to groupings were collected and diluted with 0.25% strontium chloride into 5 ml for further analysis by a fast sequential atomic absorption spectrometer. All reagents used were of analytical grade and were purchased from Merck. All containers were soaked with 20% nitric acid, rinsed with water, and then dried in a clean room for later use.

RNA Interference—Lentiviruses carrying short hairpin RNA (shRNA)-EGFP for silencing rat TRPM7 were synthesized and packaged by GeneChem Inc. Sequences identical to rat TRPM7 (GeneID 679906) but that do not match other sequences in GenBank™ were used. The DNA target sequences of the annealed double strand shRNA that we used were as follows: 5′-AACCGGAGGTCAGGTCGAAAT-3′. shRNA, with a nonsilencing oligonucleotide sequence (nonsilencing shRNA)/EGFP that does not recognize any known homology to mammalian genes, was also generated as a negative control. Cells were seeded at a density of 2×10^5, 5×10^4, or 1×10^4 cells/well in 6-well plates, coverslips in 24-well plates, or 96-well plates and grown in 2, 0.5, or 0.1 ml of Neurobasal medium supplemented with 2% B-27 medium, respectively. We got the multiplicity of infection (the appropriate ratio of the number of lentivirus to cells) value of lentivirus carrying shRNA from the preliminary experiment. Briefly, 5 or 6 days after culture, cells seeded equivalently in the 96-well plates were infected with different concentrations of lentivirus carrying shRNA. 12 h later, the cell medium was changed to freshly prepared medium. After 3 or 4 days, the fluorescence of the EGFP was detected by an inverted fluorescence microscope (Olympus IX71, Germany) to choose the best lentivirus concentration for infection. The multiplicity of infection value of shRNA/TRPM7 and shRNA/control lentivirus was 10. Then 2×10^6 or 5×10^5 transducing units of lentivirus were added to cells seeded in 6-well plates (containing 1 ml of culture medium) or coverslips in 24-well plates (containing 0.5 ml of culture medium). After mixing gently, the cell medium was changed to freshly prepared medium in 8–12 h. 3 or 4 days later, an inverted fluorescence microscope was used to detect the infection efficiency of the lentivirus. Gene silencing of TRPM7 was monitored at the mRNA and protein levels by RT-PCR and Western blot, respectively.

RT-PCR—Expression of the *TRPM7* gene was studied by RT-PCR. Primers for rat TRPM7 are detailed in the Table 1. Total RNA was extracted from cells (TRIzol reagent). RT-PCRs were performed by the RT-PCR kit (ReverTraAce Dash™, Toyobo, Japan) according to the manufacturer's instructions. Two microliters of the resulting cDNA mixture was amplified using specific primers (Table 1). TRPM7 amplification by PCR was done as follows: 95 °C for 3 min, 30 cycles of 95 °C for 60 s, 55 °C for 40 s, 72 °C for 60 s, and extension for 10 min at 72 °C. Glyceraldehyde-3-phosphate dehydrogenase amplification by PCR was done as follows: 95 °C for 3 min, 30 cycles of 94 °C for 30 s, 57 °C for 30 s, 72 °C for 45 s, and extension for 10 min at 72 °C.

TABLE 1

Primer sequence for TRPM7, G3PDH amplification by RT-PCR in rat

S indicates sense; AS indicates antisense. G3PDH is glyceraldehyde-3-phosphate dehydrogenase.

Rat	Primer sequence	Predicted size
		bp
TRPM7	(S) 5′-CTGAAGAGGAATGACTACAC-3′	660
	(AS) 5′-ACAGGGAAAAAGAGAGGGAG-3′	660
G3PDH	(S) 5′-TTGTTGCCATCAACGACCCC-3′	435
	(AS) 5′-ATGAGCCCTTCCACAATGCC-3′	435

Amplification products were electrophoresed on 1.5% agarose gel containing Glodview (0.5 μg/ml). Bands corresponding to RT-PCR products were visualized by UV light and digitized using YLN2000 gel imaging scanning system (Beijing YLN Inc.). Band intensity was quantified using the Quantity One (Bio-Rad) software.

Immunoblotting—Total protein was extracted from neurons as we described previously (14). Briefly, cells were washed with cold PBS and then harvested in lysis buffer containing 0.1% SDS, 50 mM Tris (pH 7.4), 150 mM NaCl, 1% Nonidet P-40, 0.5% sodium deoxycholate, 1% Triton X-100, 1% deoxycholate, 1 mmol/liter phenylmethylsulfonyl fluoride (PMSF). Cells were disrupted by brief sonication. After centrifugation at 12,000 × *g* at 4 °C for 30 min, the lysates were collected. The aliquots were then mixed with Laemmli sample buffer, boiled at 100 °C for 5 min, and then placed into the ice immediately to make the protein degenerate. The samples were resolved by 7.5% SDS-PAGE, followed by electrotransfer to polyvinylidene difluoride membranes. Nonspecific binding sites were blocked with 5% skim milk in Tris-buffered saline solution with Tween (TBS-T) (1 h at room temperature). For visualization, membranes were incubated with anti-TRPM7 antibody (1:200; Alomone Inc., Israel) and β-actin (1:4000; Santa Cruz Biotechnology) in TBS-T/milk at 4 °C overnight with agitation. Washed membranes were incubated with horseradish peroxidase-conjugated second antibody (1:8000; Cell Signaling) in TBS-T/milk (1 h at room temperature) and an ECL kit (GE Healthcare). The intensity of the protein band was densitometrically quantified using Quantity One (Bio-Rad) software.

Immunocytofluorescence—Cells seeded on the coverslips were gently washed twice with PBS pre-heated to 37 °C and fixed with cold 4% paraformaldehyde for 20 min. After cells were washed three times with PBS for 15 min, 10% Triton X-100 was added to rupture the cell membrane for 10 min. Again, cells were washed by PBS for 15 min; 5% bovine serum albumin was used to block the nonspecific binding sites for another 40 min. The cells were then incubated with goat polyclonal TRPM7 antibody (1:100; Santa Cruz Biotechnology) or normal goat IgG as negative control in 5% bovine serum albumin at 4 °C overnight. Washed cells were incubated with rhodamine-conjugated second antibody (1:100; Cell Signaling) in 5% bovine serum albumin (37 °C, 1 h) and Hoechst 33258 (10 μg/ml, Invitrogen) at room temperature for 10 min. Zeiss double-photon fluorescence microscope (Zeiss 510 Meta, Germany) was used to detect the fluorescence. EGFP, rhodamine, and Hoechst 33258 were excited by light of 488,543,405 nm and fluorescence emission was measured at 514,640,477 nm, respectively.

Whole Cell Patch Clamp—The whole cell patch clamp recording was performed as described previously (25). 3–4 days after

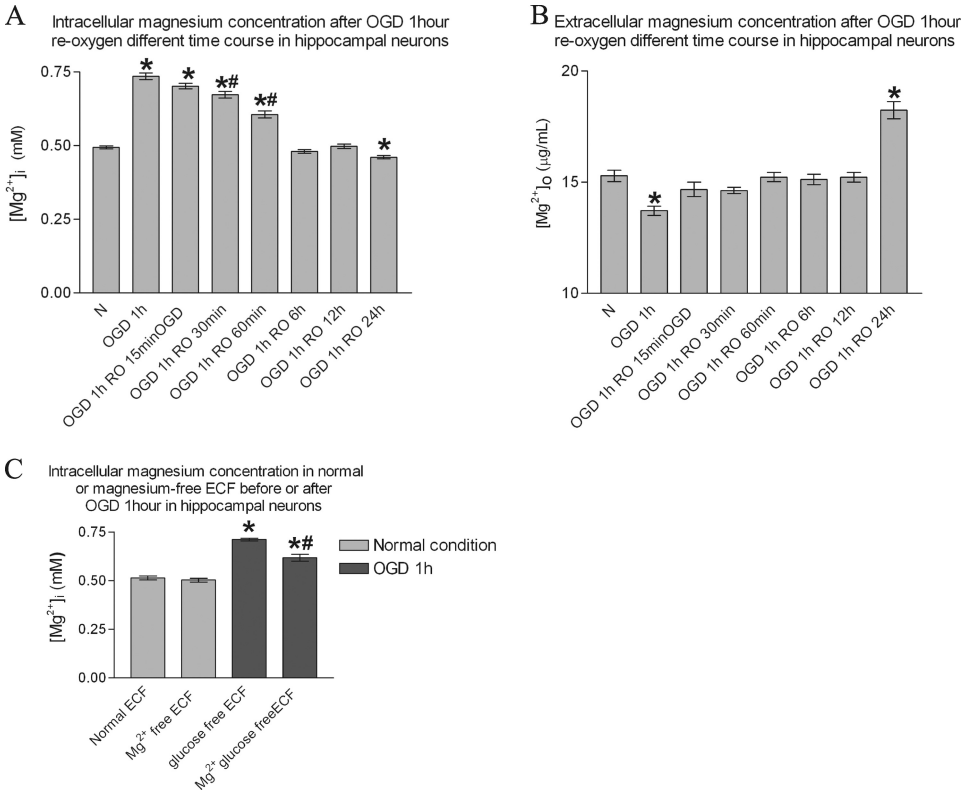

FIGURE 1. **Extracellular magnesium moving inside induced $[Mg^{2+}]_i$ increased in rat hippocampal neurons in oxygen-glucose deprivation/reperfusion.** *A,* summary *bar graph* showing the $[Mg^{2+}]_i$ of 1 h OGD following a different reperfusion time course. Neurons seeded in coverslips in 24-well plates were loaded by Mag-Fura-2 in the normal condition ($n = 72$, randomly detected cell number from four separate experiments) and after 1 h OGD (65), 1 h OGD and Re 15 min (49), 30 min (62), and 60 min (61) and 6 h (74), 12 h (68), and 24 h (84) to test $[Mg^{2+}]_i$. Data on the *ordinate* were the average $[Mg^{2+}]_i$ of each group expressed as means ± S.E. * represents having a significant difference ($p < 0.05$) compared with the normal group; # represents having a significant difference ($p < 0.05$) compared with 1 h OGD. *B,* summary *bar graph* showing the $[Mg^{2+}]_o$ of 1 h OGD following a different reperfusion time course. The extracellular liquid (500 μl/24-well plates) was acquired before OGD and immediately after 1 h OGD, 1 h OGD and Re 15, 30, and 60 min and 6, 12, and 24 h to test $[Mg^{2+}]_o$ (four samples per group, repeated three times). Data on the *ordinate* are the average $[Mg^{2+}]_o$ of each group expressed as means ± S.E. * represents having a significant difference ($p < 0.05$) compared with the normal group. *C,* summary *bar graph* showing the $[Mg^{2+}]_i$ change when removing extracellular magnesium before 1 h OGD. Randomly detected neuron numbers from each group are about 40 from three separate experiments. * represents having significant difference ($p < 0.05$) compared with the normal ECF group; # represents having significant difference ($p < 0.05$) compared with the glucose-free ECF group in OGD.

transfection, hippocampal neurons were set on the stage of the microscope at room temperature using an Axopatch 700B amplifier (Axon Instruments, Union City, CA). Patch electrodes were fabricated from borosilicate capillary tubing using a PUL-2 (WPI) micropipette puller. The resistance was around 3–5 megohms when filled with Mg^{2+}-free internal solution. Cells were bathed in external solution. Currents were filtered at 2 kHz digitized at 10 kHz by using a Digidata 1440 data acquisition system (Molecular Devices). According to the previous work, 1 mM tetrodotoxin and 5 mM nimodipine were used to block voltage-gated Na^+ and Ca^{2+} channels. TRPM7-like current was generated with a 2-s voltage ramp from −100 to +100 mV, and the holding potential was set at −60 mV, unless otherwise indicated.

Statistical Analysis—Data were expressed as means ± S.E. Groups were compared using one-way analysis of variance followed by Dunnett's test or unpaired Student's *t* test as appropriate. $p < 0.05$ was regarded as statistically significant.

RESULTS

OGD or CI Induces the Increase of Mag-Fura-2 Fluorescence Intensity That May Reflect $[Mg^{2+}]_i$ in Rat Hippocampal Neurons—We first examined whether OGD/reperfusion or CI, which mimics the condition of brain ischemia (12, 27), affects the intracellular magnesium in cultured rat hippocampal neurons using a magnesium indicator Mag-Fura-2. For finding the time window when $[Mg^{2+}]_i$ was altered in OGD/reperfusion, groups were divided into normal, 1 h OGD, 1 h OGD/reperfusion 15 min (1 h OGD and Re 15 min), 1 h OGD and Re 30 min, 1 h OGD and Re 60 min, 1 h OGD and Re 6 h, 1 h OGD and Re 12 h, and 1 h OGD and Re 24 h. As shown in Fig. 1*A*, $[Mg^{2+}]_i$ in hippocampal neurons changed from basal level 0.49 ± 0.005 mM (calculated from 72 cells) to 0.74 ± 0.01 mM after 1 h OGD ($p < 0.05$). The increase lasted for a further 60 min within reperfusion. When neurons were reperfused for 30 min following 1 h OGD, the $[Mg^{2+}]_i$ increase was on the decline but still above the basal level. Neuronal $[Mg^{2+}]_i$ recovered to normal after cells were reperfused for 6 or 12 h following 1 h OGD. Conversely, $[Mg^{2+}]_i$ in neurons was 0.46 ± 0.005 mM, slightly below the basal level after cells were reperfused for 24 h ($p < 0.05$).

Involving CI, 3 mM KCN was added when Mag-Fura-2 fluorescence was stable for a time (about 120 s) to reflect the basal level of $[Mg^{2+}]_i$. The 120-s Mag-Fura-2 fluorescence images were the images taken prior to the addition of KCN in Fig. 2*A*. Drugs were added at 120 s, which was signaled by computer, but the operation usually took less than 10 s. A sharp peak was

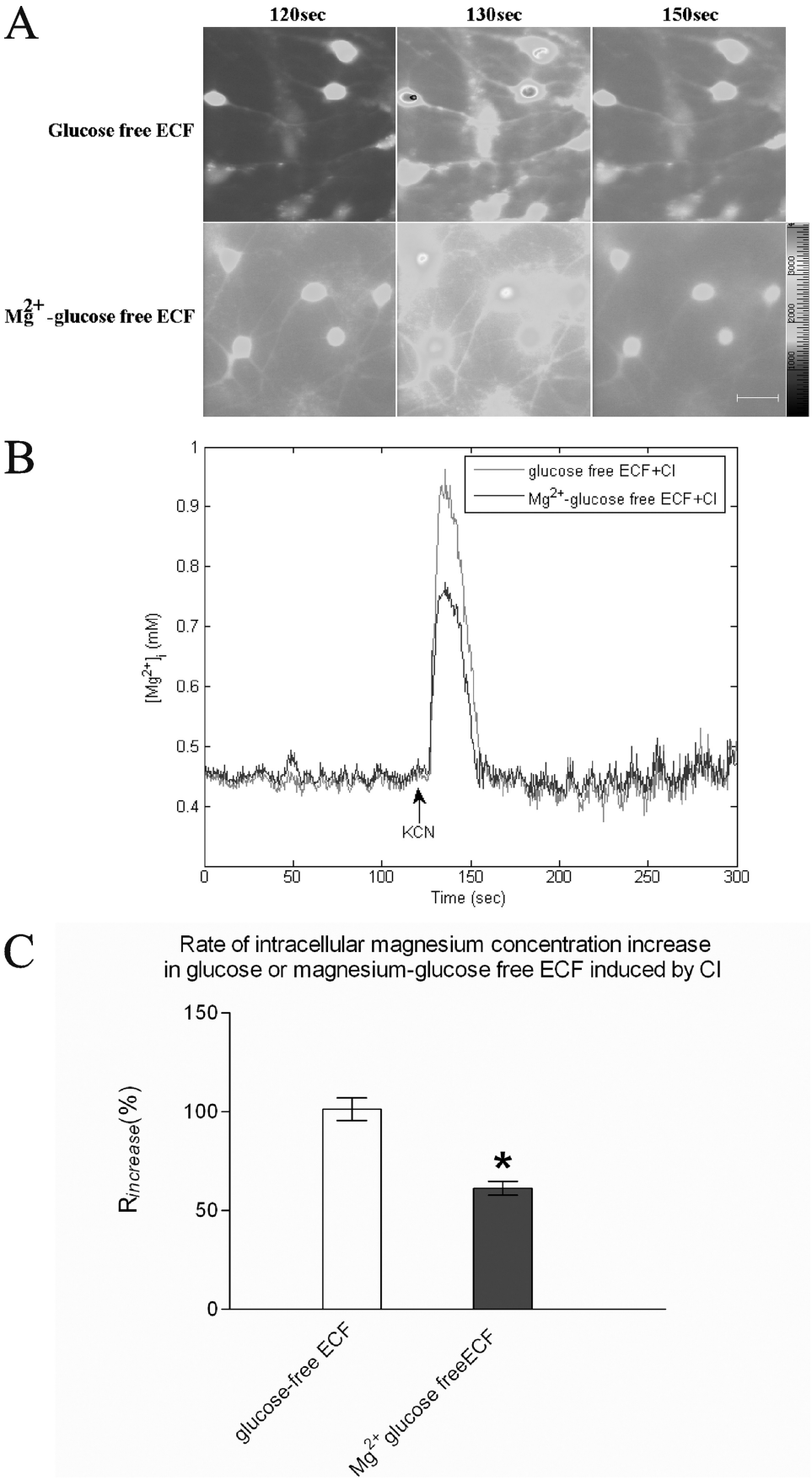
A
120sec
130sec
150sec
Glucose free ECF
Mg2+ -glucose free ECF
B
glucose free ECF+Cl
Mg2+-glucose free ECF+Cl
[Mg2+]i (mM)
KCN
Time (sec)
C
Rate of intracellular magnesium concentration increase
in glucose or magnesium-glucose free ECF induced by Cl
Rincrease(%)
glucose-free ECF
Mg2+ glucose freeECF

detected as soon as KCN was added and then disappeared immediately in ~20 s, as shown in Fig. 2*B*. The rate of increase ($R_{increase}$) was calculated by Equation 2, and the $R_{increase}$ of $[Mg^{2+}]_i$ in the chemical ischemia was 101.39 ± 5.74% (Fig. 2*C*). The results suggest that oxygen-glucose deprivation/reperfusion or acute chemical ischemia induces the increase of $[Mg^{2+}]_i$, which reflected by Mag-Fura-2 fluorescence intensity in naive rat hippocampal neurons.

$$R_{increase} = (peak[Mg^{2+}]_i - basal[Mg^{2+}]_i)/basal[Mg^{2+}]_i \times 100\% \quad \text{(Eq. 2)}$$

Increased $[Mg^{2+}]_i$ Partially Originated from the Extracellular Magnesium in Neurons—We next examined whether the increased $[Mg^{2+}]_i$ in 1 h OGD and CI originated from extracellular magnesium in rat hippocampal neurons. As direct proof, we detected magnesium concentration contained in the extracellular liquid during the different time course after 1 h OGD corresponding to the previous grouping using flame atomic absorption spectrometry. The results (Fig. 1*B*) showed that $[Mg^{2+}]_o$ decreased from 15.29 ± 0.25 to 13.72 ± 0.21 μg/ml ($p < 0.05$) after 1 h OGD. When cells were reperfused for 15 min following 1 h OGD, $[Mg^{2+}]_o$ returned to the basal level, which did not correspond to the outcome of $[Mg^{2+}]_i$. $[Mg^{2+}]_o$ was maintained in the basal level for 12 h within reperfusion. Matching the changing $[Mg^{2+}]_i$, $[Mg^{2+}]_o$ was increased to 18.25 ± 0.38 μg/ml ($p < 0.05$) after cells were reperfused for 24 h. 1 h OGD group was chosen to conduct the following experiments because both $[Mg^{2+}]_i$ and $[Mg^{2+}]_o$ changed the most and correspondingly. To confirm whether and how extracellular magnesium contributes to the increase of $[Mg^{2+}]_i$ in 1 h OGD, we removed the magnesium from extracellular liquid before OGD. As shown in Fig. 1*C*, removing extracellular magnesium did not affect the base-line intensity of Mag-Fura-2 but attenuated the increase of $[Mg^{2+}]_i$ by 40.88% from 0.71 ± 0.007 to 0.62 ± 0.02 mM ($p < 0.05$), which was also above the basal $[Mg^{2+}]_i$ level. Similarly, by taking magnesium away from the extracellular liquid before 3 mM KCN was added, the basal level of $[Mg^{2+}]_i$ was not altered, but the $R_{increase}$ of $[Mg^{2+}]_i$ was reduced by 39.52% from 101.39 ± 5.74 to 61.32 ± 3.50% (Fig. 2*C*, $p < 0.05$). These results suggest 1 h OGD or CI caused extracellular magnesium to move across the plasma membrane into the intracellular space in hippocampal neurons.

Down-regulation or Inhibition of TRPM7 Attenuates the Increase of $[Mg^{2+}]_i$ in OGD or CI in Neurons—To further verify our hypothesis that TRPM7 channels contribute to magnesium accumulation induced by OGD/CI in neurons, lentivirus carrying TRPM7 shRNA/EGFP was used to determine whether knocking down the expression of TRPM7 channels reduces the increased $[Mg^{2+}]_i$ in 1 h OGD and CI. As shown in Fig. 3, *D* and *E*, cells infected with lentivirus carrying TRPM7-shRNA/EGFP (shRNA-TRPM7 neurons as brief) for 3–4 days reduced TRPM7 in mRNA and protein levels by ~60% ($p < 0.05$) as compared with cells infected with control/EGFP lentivirus (shRNA-control neurons as brief). We also examined the effect of shRNA on TRPM7 expression in neurons with immunocytofluorescence. With specific TRPM7 antibody (Fig. 3*B*), the overall staining of TRPM7 is weaker in the shRNA-TRPM7 neurons (Fig. 3*C*) *versus* shRNA-control neurons. The expression of TRPM7 mRNA or protein was reduced by 53.61 ± 2.53% ($p < 0.05$) or 42.67 ± 5.03% ($p < 0.05$) using shRNA aimed at TRPM7, respectively (Fig. 3, *D* and *E*). Silencing TRPM7 reduced not only the basal $[Mg^{2+}]_i$ but also the increased $[Mg^{2+}]_i$ caused by 1 h OGD, but adding control/EGFP lentivirus had no effect on both basal and increased $[Mg^{2+}]_i$. As shown in Fig. 4*A*, basal $[Mg^{2+}]_i$ was decreased by 14.77% from 0.51 ± 0.05 to 0.43 ± 0.01 mM ($p < 0.05$), and increased $[Mg^{2+}]_i$ caused by 1 h OGD was reduced by 24.64% from 0.72 ± 0.02 to 0.57 ± 0.02 mM ($p < 0.05$) in shRNA-TRPM7 neurons. In the other ischemic model CI, when 3 mM KCN was added, the $R_{increase}$ of $[Mg^{2+}]_i$ in shRNA-TRPM7 neurons was lowered by 25.85% from 100.89 ± 1.69 to 76.70 ± 1.44% (Fig. 4*D*, $p < 0.05$). There was no obvious change in $R_{increase}$ of shRNA-control neurons. These results implied that TRPM7 is involved in intracellular magnesium accumulation induced by 1 h OGD or CI in neurons.

Consistent with an involvement of TRPM7 channels, addition of Gd^{3+} and 2-APB, nonspecific inhibitors of TRPM7 channels (12, 30, 31), compared with addition of DMSO, attenuated CI-induced $[Mg^{2+}]_i$ increase by 20.68 and 19.9%, respectively (Fig. 5*E*). These two drugs did not influence the base line of $[Mg^{2+}]_i$. The effect of TRPM7 inhibitors was also detected in the OGD model. As shown in Fig. 5*A*, by adding 2-APB, the basal $[Mg^{2+}]_i$ was not altered but the increased $[Mg^{2+}]_i$ caused by 1 h OGD was reduced by 18.67% from 0.72 ± 0.01 to 0.68 ± 0.01 mM ($p < 0.05$). Corresponding to the change of $[Mg^{2+}]_i$, $[Mg^{2+}]_o$ tested by flame atomic absorption spectrometry was increased from 13.53 ± 0.20 to 14.46 ± 0.17 μg/ml ($p < 0.05$) after the addition of 2-APB after 1 h OGD (Fig. 5*B*). The results suggest that TRPM7 channels play an important role in the magnesium ion homeostasis and $[Mg^{2+}]_i$ increase induced by 1 h OGD/CI in rat hippocampal neurons.

TRPM7 shRNA Reduced TRPM7-like Current—We used whole cell patch clamp to examine the effect of shRNA on TRPM7-like current in neurons. We first tested TRPM7-like currents (I_{TRPM7}) in control hippocampal neurons. As in Fig.

FIGURE 2. **Extracellular magnesium moving inside induced $[Mg^{2+}]_i$ increased in rat hippocampal neurons in acute chemical ischemia.** *A,* representative images showing changes of Mag-Fura-2 fluorescence induced by CI at the conditions indicated. KCN was added at 120 s. The 120-s Mag-Fura-2 fluorescence images were the images taken prior to the addition of KCN in *A*. Drugs were added at 120 s, which was signaled by computer, but the operation usually took less than 10 s. The *bar* in the *right corner* represents 50 μm. *B,* representative traces showing time-dependent changes of Mag-Fura-2 fluorescence that were converted to $[Mg^{2+}]_i$. KCN was added at 120 s as the *arrow* directed when Mag-Fura-2 fluorescence was stable. Each *trace* represents an average fluorescent intensity from randomly selected 10–11 cells in an experiment. *C,* summary *bar graph* showing the $[Mg^{2+}]_i$ at the 130-s time point in the different conditions indicated. $n = 30–42$ cells from three independent experiments. * represents having a significant difference ($p < 0.05$) compared with glucose-free ECF group.

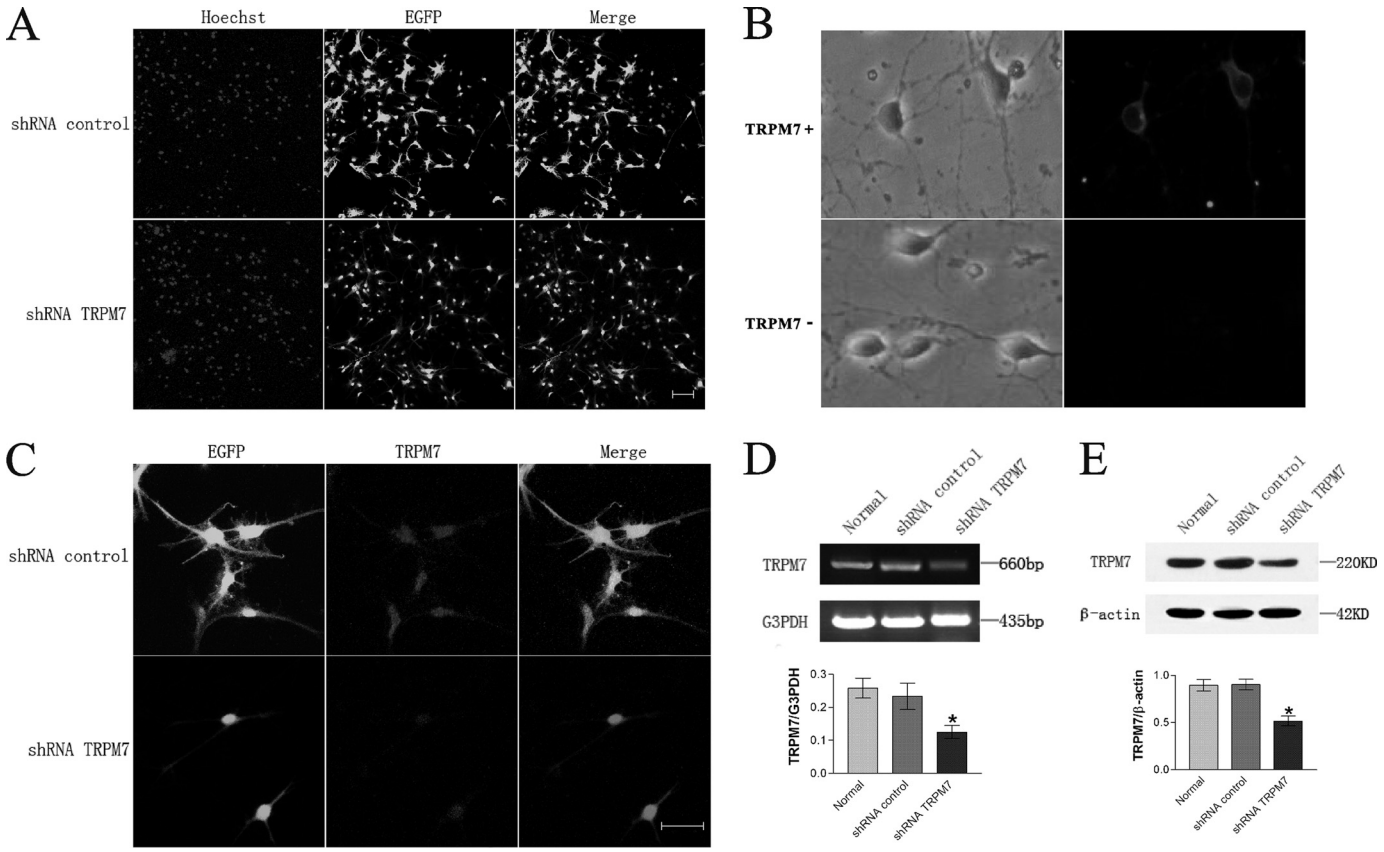

FIGURE 3. **Silencing TRPM7 with shRNA down-regulates the expression of TRPM7.** *A* shows the infection efficiency of lentivirus carrying shRNA-EGFP/TRPM7 and shRNA-EGFP/Control. Hoechst 33258 was used to dye the cell nucleus. shRNA/TRPM7 lentivirus could infect ~60% neurons, whereas shRNA/control infected ~80%. The *bar* in the *right corner* represents 100 μm. *B* shows the specificity of TRPM7 antibody. The *upper* and *lower images* represent cells stained with goat polyclonal TRPM7 antibody and normal goat IgG, respectively. The *bar* in the *right corner* represents 25 μm. *C* shows the effect of shRNA on TRPM7 expression in neurons with immunocytofluorescence. The *bar* in the *right corner* represents 50 μm. *D* shows the effect of shRNA on TRPM7 in mRNA levels using RT-PCR (averaged from five independent experiments). The mRNA of TRPM7 was reduced by 53.61 ± 2.53% using shRNA aimed at TRPM7. * represents having significant difference ($p < 0.05$) compared with the normal group. *E* shows the effect of shRNA on TRPM7 in protein level using Western blotting (averaged from three independent experiments). TRPM7 expression was reduced by 42.67 ± 5.03% shRNA aimed at TRPM7. * represents having significant difference ($p < 0.05$) compared with the normal group.

6*A*, I_{TRPM7} exhibited outward rectifying characteristics with low Ca^{2+} and no added Mg^{2+} solution when divalent cation-free solution was applied, and the inward component was preferentially enhanced over the outward component, so rectification of I_{TRPM7} was almost abolished. Substitution of NaCl by equimolar choline chloride in bath solution drastically reduced the enhanced inward current, which suggests the existence of Na^+ influx in the absence of external Mg^{2+} and Ca^{2+}. We next examined the role of Gd^{3+}, which was found to inhibit the TRPM7-mediated current. Fig. 6*B* shows relative currents recorded in the presence or absence of external divalent cations. Both inward and outward components of I_{TRPM7} were markedly enhanced in the absence of divalent cations compared with the current in the presence of external divalent ions (26.42% at +100 mV and 839.47% at −100 mV, $n = 5, p < 0.05$), and perfusion with Gd^{3+} (10 μmol/liter) in the absence of divalent cations obviously suppressed the inward current by 26.42% and outward current by 73.57% ($n = 5$, $p < 0.05$). We then compared current density between neurons treated with $shRNA_{Control}$ and $shRNA_{TRPM7}$ with low Ca^{2+}, no added Mg^{2+} bath solution. RNA interference of TRPM7 suppressed I_{TRPM7} without altering its outward rectification characteristic as in Fig. 6*C*; the inward and outward components of I_{TRPM7} in cells interfered with $shRNA_{TRPM7}$ ($n = 9$) and decreased 57.3% (−5.84 ± 0.43 for $shRNA_{control}$ *versus* −2.49 ± 0.74 for $shRNA_{TRPM7,}$ $p < 0.05$) and 73.17% (67.44 ± 9.60 for $shRNA_{control}$ *versus* 18.09 ± 4.29 for $shRNA_{TRPM7,}$ $p < 0.05$), respectively, compared with those infected with $shRNA_{control}$ (Fig. 6*D*, $n = 4$).

Overexpression of TRPM7 Channels Enhances the Increase of $[Mg^{2+}]_i$ in OGD/CI in HEK293 Cells—To provide further evidence supporting the contribution of TRPM7 channels to magnesium accumulation in 1 h OGD/CI, we investigated if changing the expression level of TRPM7 channels influences the $[Mg^{2+}]_i$ increase induced by OGD/CI. Magnesium imaging was performed in HEK293 cells. We used HEK293 cells with inducible expression of TRPM7 channels (26, 31). The expression of TRPM7 protein in HEK293 Tet(+) cells was 1.58-fold more than Tet(−) cells ($p < 0.05$) (Fig. 7*A*). As shown in (Fig. 7*C*), in the absence of induced expression of TRPM7 channels (Tet(−) cells), $[Mg^{2+}]_i$ increased from the basal level 0.41 ± 0.01 to 0.49 ± 0.01 mM ($p < 0.05$) after 1 h OGD. However, when overexpression of TRPM7 channel was induced by adding tetracycline (Tet(+) cells), the basal level of $[Mg^{2+}]_i$ of HEK293 cells increased to 0.51 ± 0.01 mM ($p < 0.05$) and was further raised to 0.56 ± 0.01 mM ($p < 0.05$) after 1 h OGD. Following

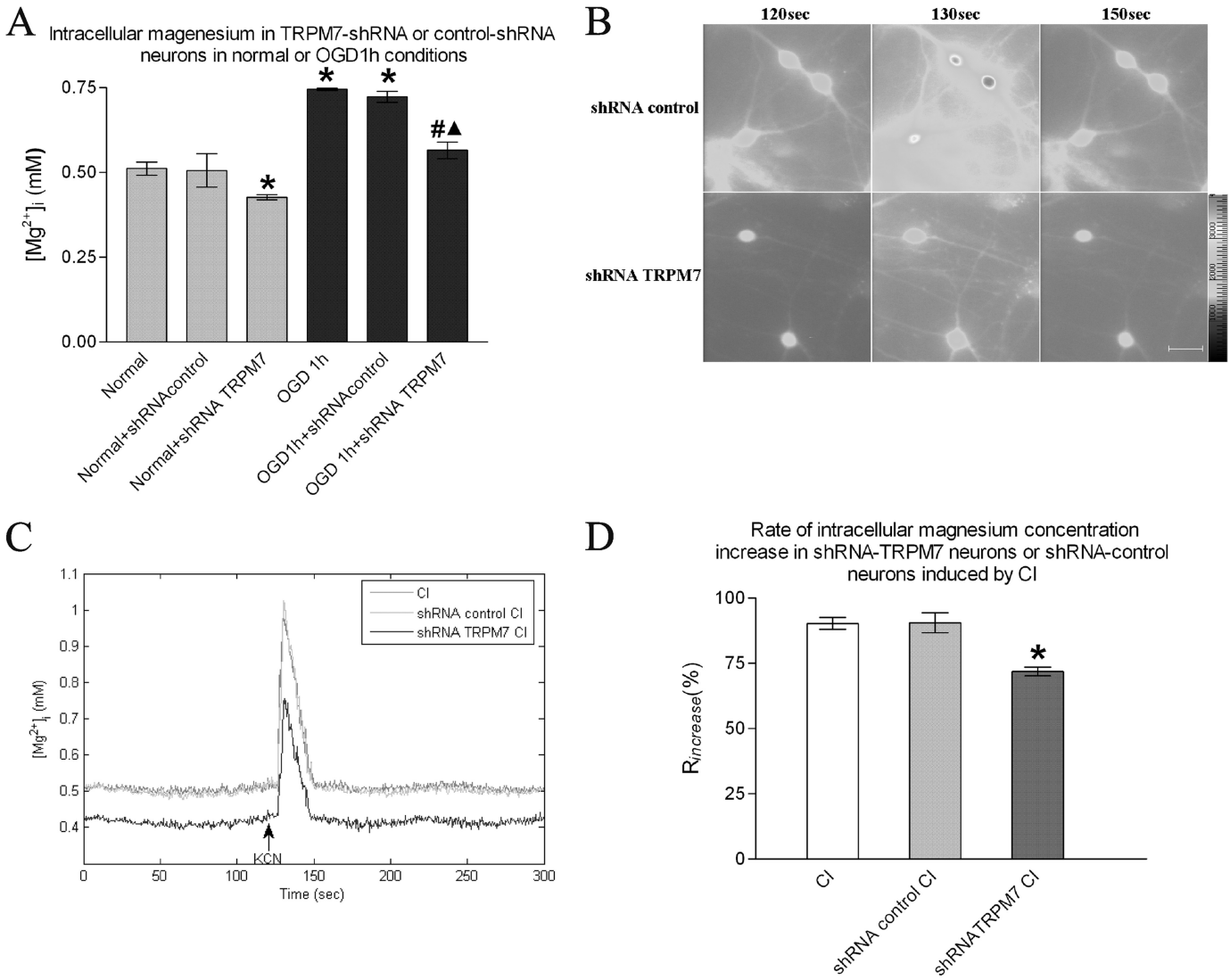

FIGURE 4. **Silencing TRPM7 with shRNA attenuates the increase of $[Mg^{2+}]_i$ in 1 h OGD or CI in neurons.** *A,* summary *bar graph* showing the $[Mg^{2+}]_i$ in TRPM7-shRNA neurons or control shRNA neurons in normal or 1 h OGD conditions. Randomly detected neuron number of each group is about 32–50 from three separate experiments. * represents having significant difference ($p < 0.05$) compared with the normal group; # represents having significant difference ($p < 0.05$) compared with the normal + shRNA TRPM7 group; ▲ represents having significant difference ($p < 0.05$) compared with the 1 h OGD group. *B,* representative images showing changes of Mag-Fura-2 fluorescence induced by CI in shRNA-TRPM7 neurons or shRNA-control neurons. KCN was added at 120 s. The 120-s Mag-Fura-2 fluorescence images were the images taken prior to the addition of KCN. The *bar* in the *right corner* represents 50 μm. *C,* representative traces showing time-dependent changes of Mag-Fura-2 fluorescence, which was converted to $[Mg^{2+}]_i$. KCN was added at 120 s as the *arrow* directed when Mag-Fura-2 fluorescence was stable. Each *trace* represents an average fluorescent intensity from randomly selected 9–14 cells in an experiment. *D,* summary *bar graph* showing the $[Mg^{2+}]_i$ at the 130-s time point in the different shRNA neurons indicated. $n = 38–52$ cells from three to four independent experiments. * represents having significant difference ($p < 0.05$) compared with CI group.

addition of KCN to mimic the acute ischemia, the $R_{increase}$ of Tet(−) cells was 36.73 ± 1.69% and the $R_{increase}$ of Tet(+) cells was lowered by adding Gd^{3+} or 2-APB (Fig. 7*F*). Addition of Gd^{3+} or 2-APB did not affect the base-line fluorescence of Mag-Fura-2 (data not shown). The $[Mg^{2+}]_i$ peak disappeared in ~100 s, which was five times longer than that of hippocampal neurons. These outcomes suggest that the level of $[Mg^{2+}]_i$ is largely determined by the level of TRPM7 channel expression in the physical condition or OGD/CI, further supporting a role of TRPM7 channels in an OGD/CI-induced $[Mg^{2+}]_i$ increase in HEK293 cells. We also observed extracellular Zn^{2+} concentration in hippocampal neuron cultures reduced after 1 h OGD and increased after 24 h of reperfusion (data not shown), which was consistent with others that overexpression of TRPM7 channels in HEK293 cells increased intracellular Zn^{2+} accumulation (31).

DISCUSSION

Magnesium, the second most common intracellular cation and the most abundant intracellular divalent cation (32–34), has been shown to be neuroprotective in several experimental models of ischemic and excitotoxic brain injury (20, 21). However, other studies have failed to detect a neuroprotective effect of magnesium (22, 23). The explanation about this controversial outcome includes the different doses, forms of magnesium administration, various models of cerebral ischemia, individual diversity of animals, etc. (22). However, magnesium was applied to brain ischemia, and it will certainly affect the intracellular

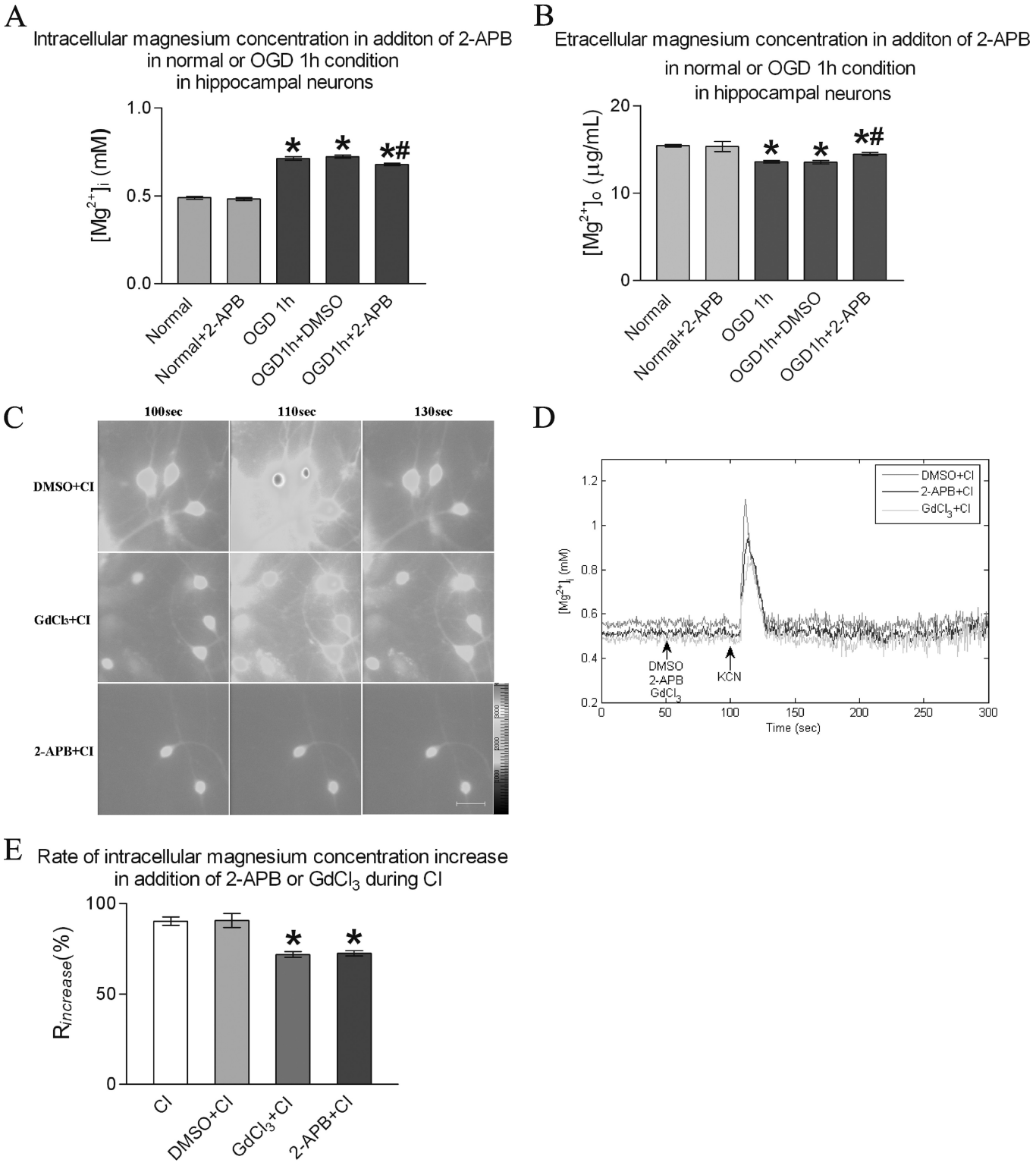

FIGURE 5. **Inhibiting TRPM7 attenuates the increase of $[Mg^{2+}]_i$ in OGD/reperfusion or CI in neurons.** *A,* summary *bar graph* showing $[Mg^{2+}]_i$ change in addition to 2-APB before 1 h OGD. 2-APB was added before 1 h OGD and thus affected the whole OGD process. $n = 39–49$ randomly selected neurons from three separate experiments. * represents having significant difference ($p < 0.05$) compared with normal group; # represents having significant difference ($p < 0.05$) compared with 1 h OGD group. *B* shows $[Mg^{2+}]_o$ change in addition to 2-APB before 1 h OGD (four samples per group and repeated three times). * represents having a significant difference ($p < 0.05$) compared with the normal group; # represents having significant difference ($p < 0.05$) compared with the 1 h OGD group. *C* shows the typical images of neurons loaded by Mag-Fura-2 in three time phases of CI in addition of 2-APB or Gd^{3+}. 100 μM 2-APB or 10 μM Gd^{3+} was added at 50 s when fluorescence of Mag-Fura-2 was stable following KCN at 100 s. The 100-s Mag-Fura-2 fluorescence images were the images taken prior to the addition of KCN. The *bar* in the *right corner* represents 50 μm. *D,* representative traces showing time-dependent changes of Mag-Fura-2 fluorescence that were converted to $[Mg^{2+}]_i$ in addition of 2-APB or Gd^{3+} during CI. 100 μM 2-APB or 10 μM Gd^{3+} was added at 50 s when fluorescence of Mag-Fura-2 was stable following KCN at 100 s as the *arrow* directed. Each *trace* represents an average fluorescent intensity from randomly selected 10–12 cells in an experiment. *E,* summary *bar graph* showing the $[Mg^{2+}]_i$ at the 110-s time point in the different conditions indicated. $n = 34–46$ cells from an independent experiment that was repeated four times. * represents having significant difference ($p < 0.05$) compared with the CI group.

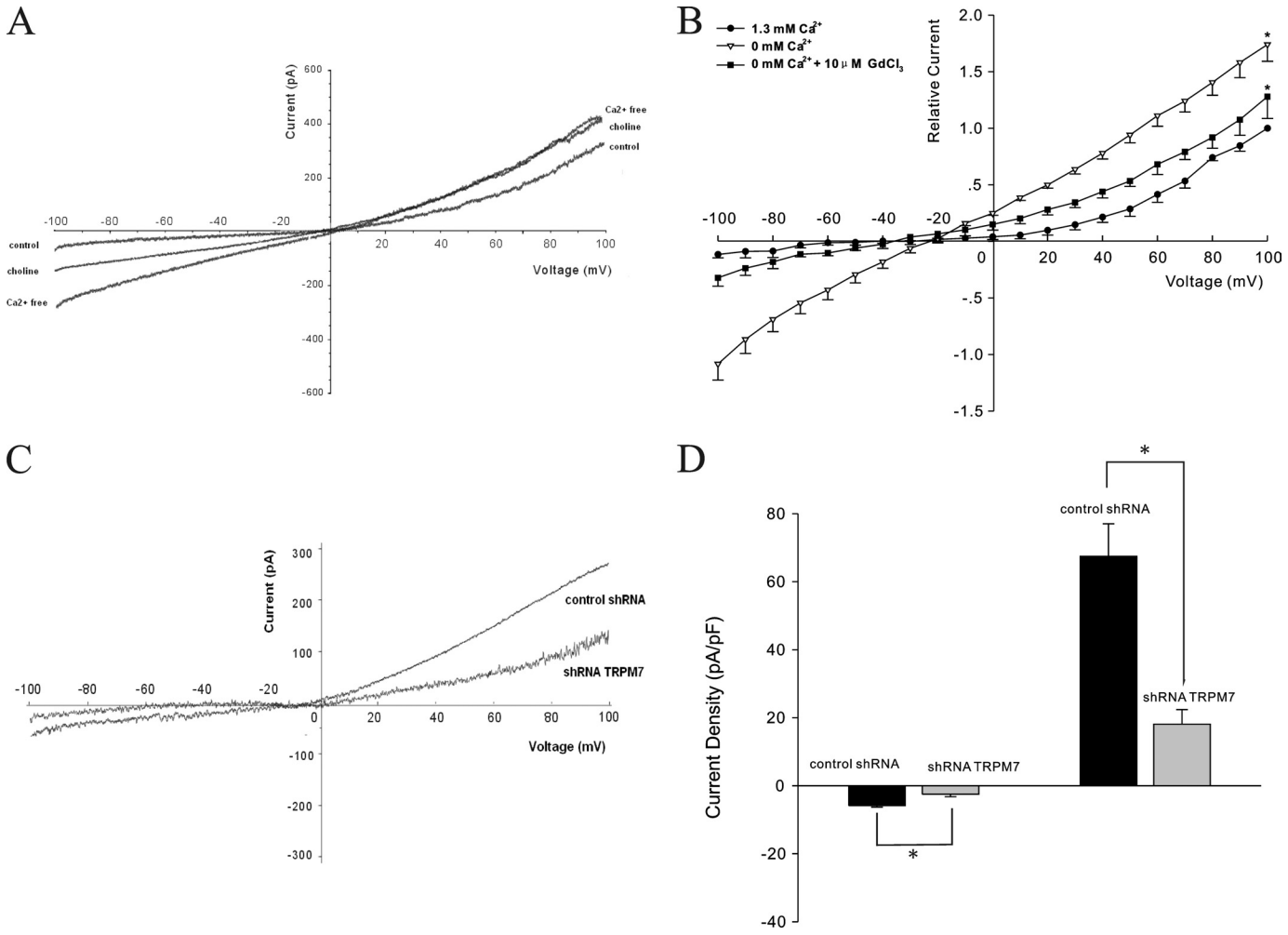

FIGURE 6. **TRPM7-like current and the effect of infection with shRNA$_{TRPM7}$.** *A,* typical currents of a control neuron perfused with low Ca^{2+}, no added Mg^{2+} solution, divalent cation-free external solution, or choline-substituted Na^{+}-free external solution without divalent cations. *B,* reduction of the relative outwardly rectifying current recorded in control neuron by 10 μmol/liter Gd^{3+}; all values at different points were normalized to the response induced by voltage ramp in low Ca^{2+}, no added Mg^{2+} solution ($n = 5$, *, $p < 0.05$). *C,* typical currents of neurons treated with shRNA$_{Control}$ and shRNA$_{TRPM7}$. *D,* decrease in current density of shRNATRPM7 treated neurons *versus* control ($n = 9$ for shRNA$_{control}$, $n = 4$ for shRNA$_{TRPM7}$; *, $p < 0.05$).

magnesium. So, it is very necessary to research the intracellular magnesium dynamic pattern in cerebral ischemia. Because of the complicated impact that exists *in vivo*, we chose cultured primary hippocampal neurons, which were reported highly sensitive to anoxia (1), to carry out the experiments. We detected the $[Mg^{2+}]_i$ in neurons by loading cells with Mag-Fura-2/AM fluorescent dye. It showed that the basal level of $[Mg^{2+}]_i$ was 0.49 ± 0.005 mM ($n = 72$), which is similar to other reports (29, 35, 36). $[Mg^{2+}]_i$ is 1.51-fold as high as the basal level after 1 h of OGD. The increase achieved the peak just after 1 h of OGD and was kept on for 60 min within reperfusion. Conversely, $[Mg^{2+}]_i$ in neurons decreased slightly below the basal level after cells were reperfused for 24 h. Following addition of KCN, the $[Mg^{2+}]_i$ peak (increasing rate is 101.39 ± 5.74%) immediately appeared. Both results told us that there may be a Mg^{2+} overload inside the neurons induced by hypoxia. It had been reported that depolarization triggers an intracellular magnesium surge in cultured dorsal root ganglion neurons (37), which supported our research because hypoxia may induce cellular potential depolarization (2). There are still a lot of studies about the $[Mg^{2+}]_i$ change in traumatic brain injury (38) showing the sustained decline in intracellular free magnesium concentration, which may be due to the different pathological processes between these two kinds of brain injury, which await clarification.

Intracellular magnesium is tightly regulated by precise control mechanisms at the level of magnesium entry, magnesium efflux (28, 29, 39), intracellular buffering (40, 41), and compartmentalization (42, 43). Therefore, we further tested $[Mg^{2+}]_o$ of different reperfusion phases after 1 h OGD. What we found was that $[Mg^{2+}]_o$ decreased only after 1 h OGD and recovered to the pre-ischemic level within 15 min after reperfusion. Similar research carried out *in vivo* (44) showed that $[Mg^{2+}]_o$ significantly decreased to 41% of base line during cerebral ischemia and gradually returned to 67% of base line after 60 min of reperfusion. These results corresponded to our $[Mg^{2+}]_i$ changing rule but were not consistent with the $[Mg^{2+}]_o$ changing rule in the reperfusion part. This may be affected by some other elements *in vivo*, such as glia cells, humoral factors, etc., which need to be clarified. The outcome here implied the $[Mg^{2+}]_i$ accumulation after 1 h OGD partially originated from $[Mg^{2+}]_o$, and accumulation within 60 min after reperfusion may mainly

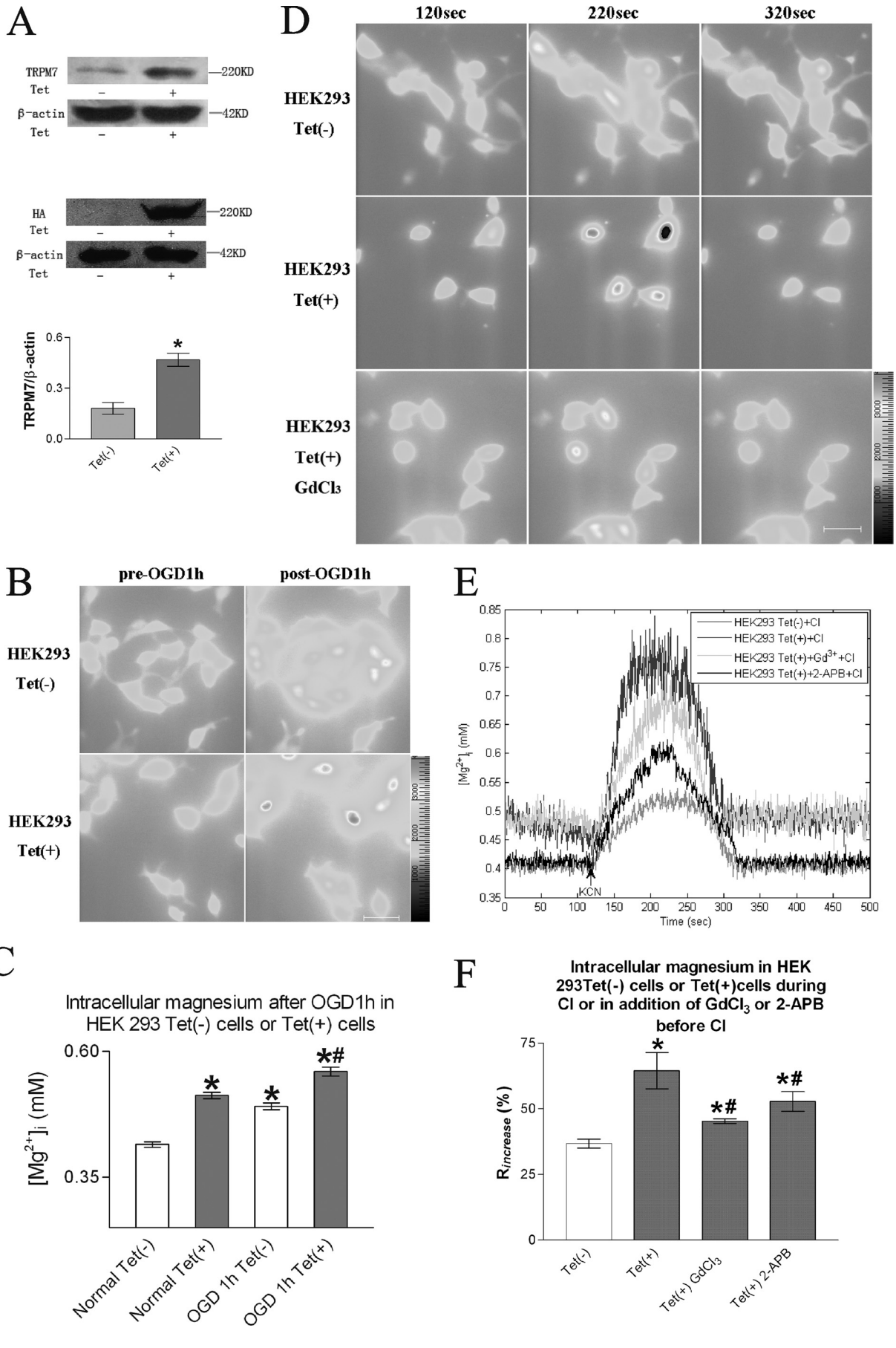
A
TRPM7
Tet
220KD
β-actin
42KD
HA
TRPM7/β-actin
Tet(-)
Tet(+)
B
pre-OGD1h
post-OGD1h
HEK293 Tet(-)
HEK293 Tet(+)
C
Intracellular magnesium after OGD1h in HEK 293 Tet(-) cells or Tet(+) cells
[Mg2+]i (mM)
Normal Tet(-)
Normal Tet(+)
OGD 1h Tet(-)
OGD 1h Tet(+)
D
120sec
220sec
320sec
HEK293 Tet(-)
HEK293 Tet(+)
HEK293 Tet(+) GdCl3
E
HEK293 Tet(-)+Cl
HEK293 Tet(+)+Cl
HEK293 Tet(+)+Gd3+ +Cl
HEK293 Tet(+)+2-APB+Cl
[Mg2+]i (mM)
KCN
Time (sec)
F
Intracellular magnesium in HEK 293Tet(-) cells or Tet(+)cells during Cl or in addition of GdCl3 or 2-APB before Cl
Rincrease (%)
Tet(-)
Tet(+)
Tet(+) GdCl3
Tet(+) 2-APB

resulted from the mechanisms inside the neurons as follows: depletion of intracellular ATP/GTP (40) and release from mitochondrion (43) induced by anoxic insults, etc. To further confirm, we removed extracellular magnesium and found the $[Mg^{2+}]_i$ increase after 1 h OGD declined by 40.88% and the $[Mg^{2+}]_i$ peak in CI by 39.52%. The results suggest that the increase by about 40% of the $[Mg^{2+}]_i$ after 1 h OGD/CI was contributed from the extracellular Mg^{2+}.

Subsequently, we focused on 1 h after OGD injury in ways in which the magnesium ions cross the neuronal cell membrane from the extracellular into the intracellular space. Transporters and exchangers that have been implicated in Mg^{2+} transport through the membrane include the following: Na^+-Mg^{2+} and Ca^{2+}-Mg^{2+} exchangers mainly for efflux of Mg^{2+} (45, 46); the human solute carrier family 41, members 1 and 2 (SLC41A1 and SLC41A2) (47, 48); ancient conserved domain protein 2 (ACDP2) (49); and magnesium transporter 1 (MagT1) (50), TRPM6, and TRPM7. With respect to the impressive involvement of TRPM7, the latest cerebral ischemia research, and the importance of TRPM7 in regulating intracellular Mg^{2+} homeostasis and $[Mg^{2+}]_i$ in a cell-specific manner (51, 52), we decided to see whether TRPM7 attends the magnesium dynamic change in 1 h OGD/CI. Silencing TRPM7 with shRNA in neurons decreased the basal $[Mg^{2+}]_i$ by 14.77%, the increase of $[Mg^{2+}]_i$ (OGD) by 24.64%, and the peak of $[Mg^{2+}]_i$ (CI) by 25.85%, respectively. Addition of Gd^{3+} or 2-APB, inhibitors of TRPM7 channels, attenuated the CI-induced $[Mg^{2+}]_i$ increase by 20.68 and 19.9%, respectively, which did not affect basal $[Mg^{2+}]_i$. $[Mg^{2+}]_i$ caused by 1 h OGD was reduced by 18.67% adding 2-APB before OGD. These outcomes suggest that about one-fourth of $[Mg^{2+}]_i$ accumulation is attributed to TRPM7 channels that provide access to extracellular magnesium moving inside. We found the different effects to basal $[Mg^{2+}]_i$ between using silencing TRPM7 protein and the TRPM7 channels inhibitors. The possible reasons may be from two major possibilities. One is the inhibiting efficiency of these two nonspecific inhibitors of TRPM7 channels. Their decreasing efficiency for increased $[Mg^{2+}]_i$ induced by OGD/CI is also lower than that of silencing the TRPM7 protein. The other is that the inhibition of Gd^{3+} or 2-APB is mainly on the TRPM7 channels, whereas silencing the TRPM7 protein is silencing the entire protein, channels, and α-kinase. It had been reported that the kinase domain of TRPM7 may mediate the regulation of the channel functions of TRPM7 (51, 53).

As further support, overexpression of TRPM7 in HEK293 cells exaggerated both the basal and increased $[Mg^{2+}]_i$ after 1 h OGD/CI. It is believed that TRPM7 contributes to the magnesium transmembrane movement in physical homeostasis maintenance and anoxia conditions to a certain extent in hippocampal neurons and HEK293 cells. Not only in these two cells, there are also data supporting TRPM7-mediated Mg^{2+} influx in cardiovascular and epithelial cells (55).

Mag-Fura-2 is widely used in $[Mg^{2+}]_i$ measurements (29, 35, 37), although Mag-Fura-2 responds to high levels of intracellular Ca^{2+} (56, 57). So we must carefully distinguish the effects of these two ions. The dissociation constant of Mag-Fura-2 for Ca^{2+} is ~30 μM (58), and the maximum value of $[Ca^{2+}]_i$ during cerebral ischemia is lower than 0.2 μM in neurons that had been reported (12, 29, 59). The correction of $[Mg^{2+}]_i$ for binding of Ca^{2+} to Mag-Fura-2 represents <50 μM $[Mg^{2+}]_i$ (60). In our studies, the $[Mg^{2+}]_i$ changed from 0.4 to 1.2 mM. As a result, it seems unlikely that the present $[Mg^{2+}]_i$ signals were due to the $[Ca^{2+}]_i$ increase in the OGD/CI.

$[Ca^{2+}]_i$ had also been detected to increase extensively during ischemic insults. The profile of $[Ca^{2+}]_i$ dynamic changes commonly observed was that $[Ca^{2+}]_i$ increased at the very beginning of OGD, and the increase lasted during the whole anoxia process and recovered to pre-ischemic levels within a short time (about 10 min) after reperfusion (12, 59). The different time phase of these two important cations implied there may be some kind of interaction. It has been reported that glutamate caused a large increase in $[Mg^{2+}]_i$ through a Ca^{2+} influx in cerebral neurons (29), and an intracellular Mg^{2+} surge followed Ca^{2+} increase during depolarization in cultured neurons (37). According to the time window differences and the reports above, it is accepted that $[Ca^{2+}]_i$ overload may contribute to the $[Mg^{2+}]_i$ overload to a certain degree in OGD/CI and that needs our further investigation. Moreover, magnesium is an important modulator of $[Ca^{2+}]_i$ through its negative modulatory effects on numerous Ca^{2+} channels (L-type, T-type, store-operated, and calcium release-activated Ca^{2+} channels) by influencing Ca^{2+}-ATPase activity, ryanodine receptors, and mobilization of intracellular Ca^{2+} reticular stores (61, 62). It may explain why that $[Ca^{2+}]_i$ overload declined just after $[Mg^{2+}]_i$ mostly increased.

TRPM7 protein consists of an ion channel, containing a magnesium-permeable pore, fused to a kinase domain at the COOH terminus, and it is thus termed a "chanzyme" (16, 17). The character of these channels, which are Mg^{2+}-permeable and Mg^{2+} is sensitively inhibited at the same time (63), provides important feedback regulating the mechanism of magnesium homeostasis. This may be part of the reason why $[Mg^{2+}]_o$ recovered so

FIGURE 7. **Overexpression of TRPM7 channels enhances the increase of $[Mg^{2+}]_i$ that is regulated by Gd^{3+} in 1 h OGD/CI in HEK293 cells.** *A* shows TRPM7 overexpression by Western blotting using anti-HA or anti-TRPM7 as the primary antibody in HEK293 Tet(−) cells or Tet(+) cells. Adding 1 μg/ml tetracycline 24 h before 1 h OGD/CI induced overexpression of TRPM7 expression. The expression of TRPM7 protein in HEK293 Tet(+) cells was 1.58-fold more than Tet(−) cells. * represents having a significant difference ($p < 0.05$) compared with the Tet(−) group. *B* shows the typical images of HEK293 Tet(−) cells or Tet(+) cells loaded by Mag-Fura-2 pre- and post-OGD as indicated. The *bar* in the *right corner* represents 50 μm. *C,* summary *bar graph* shows $[Mg^{2+}]_i$ change after 1 h OGD in HEK293 Tet(−) cells or Tet(+) cells. n = 140–153 randomly selected cells from three independent experiments. * represents having significant difference ($p < 0.05$) compared with normal Tet(−) group; # represents having significant difference ($p < 0.05$) compared with 1 h OGD Tet(−) group. *D* shows the typical images of HEK293 Tet(−) cells or Tet(+) cells loaded by Mag-Fura-2 in CI and in addition of Gd^{3+} before CI. Gd^{3+} was added at 60 s following KCN at 120 s. The 120-s Mag-Fura-2 fluorescence images were the images taken prior to the addition of KCN. The *bar* in the *right corner* represents 50 μm. *E,* representative traces showing time-dependent changes of Mag-Fura-2 fluorescence that was converted to $[Mg^{2+}]_i$ in HEK293 Tet(−) cells or Tet(+) cells during CI or Tet(+) cells in addition to Gd^{3+} before CI. Gd^{3+} or 2-APB was added at 60 s following KCN at 120 s as the *arrow* directed. Each *trace* represents an average fluorescent intensity from randomly selected 10–14 cells in an experiment. *F,* summary *bar graph* shows the $[Mg^{2+}]_i$ at the 220-s time point in the different conditions indicated. n = 39–42 cells from three independent experiment, which was repeated four times. * represents having significant difference ($p < 0.05$) compared with Tet(−) group; # represents having significant difference ($p < 0.05$) compared with the Tet(+) group.

quickly just after reperfusion, and the $[Mg^{2+}]_i$ increase in 1 h OGD/CI is not entirely attributed to TRPM7. TRPM7 channels can also permeate Ca^{2+}. The $[Ca^{2+}]_i$ overload in neurons induced by OGD/CI was mediated by TRPM7 channels as reported previously (15). So when TRPM7 channels were activated in OGD/CI, calcium may enter the neurons followed by magnesium. These two ions affected each other and finally affected the neuronal destination. The concrete relationship between these two and the results of neurons await further clarification.

Because TRPM7 kinase activity requires magnesium (64), the obvious increase of $[Mg^{2+}]_i$ induced by OGD/CI may affect neuronal destination through altering TRPM7 kinase activity to phosphate-specific substrates and then affect their signaling pathways in anoxia conditions. It had been reported that an excess amount of intracellular Mg^{2+} induced by hyperactivity of *N*-methyl-D-aspartate channels occasionally causes neuronal cell death as a result of inhibitory effects of Mg^{2+} to mitochondrial activities (24). The change of $[Mg^{2+}]_i$ in OGD/CI may also affect the cellular function in which magnesium is required as follows: maintenance of the active conformation of macromolecules, regulation of lipid- and phosphoinositide-derived second messengers, regulation of transporters and ion channels (33, 54), etc.

Acknowledgments—We thank Prof. Loren W. Runnels (University of Medicine and Dentistry of New Jersey-Robert Wood Johnson Medical School) for providing eukaryotic expression plasmid containing mouse TRPM7 cDNA, pcDNA5/FRT/TO-HA-TRPM7/WT. We thank the technological support at the Public Platform of Key Laboratory of Neurological Disease of Hubei Province, especially technologist Dan Ke.

REFERENCES

1. Schwartz, P. H., Massarweh, W. F., Vinters, H. V., and Wasterlain, C. G. (1992) *Stroke* **23,** 539–546
2. Dirnagl, U., Iadecola, C., and Moskowitz, M. A. (1999) *Trends Neurosci.* **22,** 391–397
3. Choi, D. W. (1987) *J. Neurosci.* **7,** 369–379
4. White, R. J., and Reynolds, I. J. (1995) *J. Neurosci.* **15,** 1318–1328
5. Pignataro, G., Gala, R., Cuomo, O., Tortiglione, A., Giaccio, L., Castaldo, P., Sirabella, R., Matrone, C., Canitano, A., Amoroso, S., Di Renzo, G., and Annunziato, L. (2004) *Stroke* **35,** 2566–2570
6. Pisani, A., Bonsi, P., Centonze, D., Giacomini, P., and Calabresi, P. (2000) *J. Cereb. Blood Flow Metab.* **20,** 839–846
7. Loew, L. M., Carrington, W., Tuft, R. A., and Fay, F. S. (1994) *Proc. Natl. Acad. Sci. U.S.A.* **91,** 12579–12583
8. Planells-Cases, R., Lerma, J., and Ferrer-Montiel, A. (2006) *Curr. Pharm. Des.* **12,** 3583–3596
9. Davis, S. M., Lees, K. R., Albers, G. W., Diener, H. C., Markabi, S., Karlsson, G., and Norris, J. (2000) *Stroke* **31,** 347–354
10. Lees, K. R., Asplund, K., Carolei, A., Davis, S. M., Diener, H. C., Kaste, M., Orgogozo, J. M., and Whitehead, J. (2000) *Lancet* **355,** 1949–1954
11. Kalia, L. V., Kalia, S. K., and Salter, M. W. (2008) *Lancet Neurol.* **7,** 742–755
12. Aarts, M., Iihara, K., Wei, W. L., Xiong, Z. G., Arundine, M., Cerwinski, W., MacDonald, J. F., and Tymianski, M. (2003) *Cell* **115,** 863–877
13. Sun, H. S., Jackson, M. F., Martin, L. J., Jansen, K., Teves, L., Cui, H., Kiyonaka, S., Mori, Y., Jones, M., Forder, J. P., Golde, T. E., Orser, B. A., Macdonald, J. F., and Tymianski, M. (2009) *Nat. Neurosci.* **12,** 1300–1307
14. Zhao, L., Wang, Y., Sun, N., Liu, X., Li, L., and Shi, J. (2007) *Life Sci.* **81,** 1211–1222
15. Nicotera, P., and Bano, D. (2003) *Cell* **115,** 768–770
16. Monteilh-Zoller, M. K., Hermosura, M. C., Nadler, M. J., Scharenberg, A. M., Penner, R., and Fleig, A. (2003) *J. Gen. Physiol.* **121,** 49–60
17. Schlingmann, K. P., and Gudermann, T. (2005) *J. Physiol.* **566,** 301–308
18. Schlingmann, K. P., Waldegger, S., Konrad, M., Chubanov, V., and Gudermann, T. (2007) *Biochim. Biophys. Acta* **1772,** 813–821
19. Romani, A. M. (2007) *Front. Biosci.* **12,** 308–331
20. Lee, E. J., Ayoub, I. A., Harris, F. B., Hassan, M., Ogilvy, C. S., and Maynard, K. I. (1999) *J. Neurosci. Res.* **58,** 442–448
21. Miles, A. N., Majda, B. T., Meloni, B. P., and Knuckey, N. W. (2001) *Neurosurgery* **49,** 1443–1451
22. Zhu, H. D., Martin, R., Meloni, B., Oltvolgyi, C., Moore, S., Majda, B., and Knuckey, N. (2004) *Neurosci. Res.* **49,** 347–353
23. Blair, J. L., Warner, D. S., and Todd, M. M. (1989) *Stroke* **20,** 507–512
24. Sato, Y., and Fukuda, J. (2004) *Clin. Calcium* **14,** 50–57
25. Tian, S. L., Jiang, H., Zeng, Y., Li, L. L., and Shi, J. (2007) *Neurosci. Lett.* **419,** 93–98
26. Su, L. T., Agapito, M. A., Li, M., Simonson, W. T., Huttenlocher, A., Habas, R., Yue, L., and Runnels, L. W. (2006) *J. Biol. Chem.* **281,** 11260–11270
27. Goldberg, M. P., and Choi, D. W. (1993) *J. Neurosci.* **13,** 3510–3524
28. Quamme, G. A., and Rabkin, S. W. (1990) *Biochem. Biophys. Res. Commun.* **167,** 1406–1412
29. Brocard, J. B., Rajdev, S., and Reynolds, I. J. (1993) *Neuron* **11,** 751–757
30. Li, M., Jiang, J., and Yue, L. (2006) *J. Gen. Physiol.* **127,** 525–537
31. Inoue, K., Branigan, D., and Xiong, Z. G. (2010) *J. Biol. Chem.* **285,** 7430–7439
32. Altura, B. M., and Altura, B. T. (1991) *Magnes. Trace Elem.* **10,** 182–192
33. Grubbs, R. D., and Maguire, M. E. (1987) *Magnesium* **6,** 113–127
34. Rubin, H. (2007) *Arch. Biochem. Biophys.* **458,** 16–23
35. Kennedy, H. J. (1998) *Exp. Physiol.* **83,** 449–460
36. Gotoh, H., Kajikawa, M., Kato, H., and Suto, K. (1999) *Brain Res.* **828,** 163–168
37. Kato, H., Gotoh, H., Kajikawa, M., and Suto, K. (1998) *Brain Res.* **779,** 329–333
38. Heath, D. L., and Vink, R. (1996) *Brain Res.* **738,** 150–153
39. Quamme, G. A. (1997) *Kidney Int.* **52,** 1180–1195
40. Gasbarrini, A., Borle, A. B., Farghali, H., Bender, C., Francavilla, A., and Van Thiel, D. (1992) *J. Biol. Chem.* **267,** 6654–6663
41. Gabriel, T. E., and Günzel, D. (2007) *Arch. Biochem. Biophys.* **458,** 3–15
42. Romani, A., Marfella, C., and Scarpa, A. (1993) *Circ. Res.* **72,** 1139–1148
43. Crompton, M., Capano, M., and Carafoli, E. (1976) *Biochem. J.* **154,** 735–742
44. Lin, M. C., Huang, Y. L., Liu, H. W., Yang, D. Y., Lee, C. P., Yang, L. L., and Cheng, F. C. (2004) *J. Am. Coll. Nutr.* **23,** 561S-565S
45. Beyenbach, K. W. (1990) *Magnes. Trace Elem.* **9,** 233–254
46. Wolf, F. I., Di Francesco, A., Covacci, V., and Cittadini, A. (1994) *Biochem. Biophys. Res. Commun.* **202,** 1209–1214
47. Kolisek, M., Launay, P., Beck, A., Sponder, G., Serafini, N., Brenkus, M., Froschauer, E. M., Martens, H., Fleig, A., and Schweigel, M. (2008) *J. Biol. Chem.* **283,** 16235–16247
48. Sahni, J., Nelson, B., and Scharenberg, A. M. (2007) *Biochem. J.* **401,** 505–513
49. Goytain, A., and Quamme, G. A. (2005) *Physiol. Genomics* **22,** 382–389
50. Zhou, H., and Clapham, D. E. (2009) *Proc. Natl. Acad. Sci. U.S.A.* **106,** 15750–15755
51. Schmitz, C., Perraud, A. L., Johnson, C. O., Inabe, K., Smith, M. K., Penner, R., Kurosaki, T., Fleig, A., and Scharenberg, A. M. (2003) *Cell* **114,** 191–200
52. Rhian, M., and Touyz, R. M. (2008) *Am. J. Physiol. Heart Circ. Physiol.* **294,** H1103–H1118
53. Takezawa, R., Schmitz, C., Demeuse, P., Scharenberg, A. M., Penner, R., and Fleig, A. (2004) *Proc. Natl. Acad. Sci. U.S.A.* **101,** 6009–6014
54. Agus, Z. S., and Morad, M. (1991) *Annu. Rev. Physiol.* **53,** 299–307
55. He, Y., Yao, G., Savoia, C., and Touyz, R. M. (2005) *Circ. Res.* **96,** 207–215
56. Raju, B., Murphy, E., Levy, L. A., Hall, R. D., and London, R. E. (1989) *Am. J. Physiol.* **256,** C540–C548
57. Sugiyama, T., and Goldman, W. F. (1995) *Am. J. Physiol.* **269,** C698–C705
58. Haugland, R. P. (1996) *Handbook of Fluorescent Probes and Research*

Chemicals, pp. 507–510 Molecular Probes, Eugene, OR
59. Nakamura, T., Minamisawa, H., Katayama, Y., Ueda, M., Terashi, A., Nakamura, K., and Kudo, Y. (1999) *Neuroscience* **88,** 57–67
60. London, R. E. (1991) *Annu. Rev. Physiol.* **53,** 241–258
61. Wang, M., and Berlin, J. R. (2007) *Arch. Biochem. Biophys.* **458,** 65–72
62. Zhang, J., Berra-Romani, R., Sinnegger-Brauns, M. J., Striessnig, J., Blaustein, M. P., and Matteson, D. R. (2007) *Am. J. Physiol. Heart Circ. Physiol.* **292,** H415–H425
63. Nadler, M. J., Hermosura, M. C., Inabe, K., Perraud, A. L., Zhu, Q., Stokes, A. J., Kurosaki, T., Kinet, J. P., Penner, R., Scharenberg, A. M., and Fleig, A. (2001) *Nature* **411,** 590–595
64. Hermosura, M. C., Nayakanti, H., Dorovkov, M. V., Calderon, F. R., Ryazanov, A. G., Haymer, D. S., and Garruto, R. M. (2005) *Proc. Natl. Acad. Sci. U.S.A.* **102,** 11510–11515